RADIAL BASIS FUNCTIONS APPLIED TO THE SOLUTION OF THE NATURAL CONVECTION PROBLEM IN SQUARE CAVITIES

Ana C. Magalhães, ana_mag1981@hotmail.com
Marcelo J. Colaço, colaco@asme.org
Military Institute of Engineering, Dept. of Mechanical and Materials Engineering.
Praca General Tibúrcio, 80, Rio de Janeiro, RJ, 22290-270, Brazil

Helcio R. B. Orlande, helcio@mecanica.coppe.ufrj.br
Federal University of Rio de Janeiro, Dept. of Mechanical Engineering.
Cx. Postal 68503, Rio de Janeiro, RJ, 21945-970, Brazil

George S. Dulikravich, dulikrav@fiu.edu
Florida International University, Dept. of Mechanical and Materials Engineering
10555 West Flagler St., EC 3474, Miami, FL 33174, USA

Abstract. *This work deals with the application of the Radial Basis Function (RBF) to the solution of two convective-diffusive problems. The first problem is the classical lid-driven cavity flow and the second problem is the natural convection problem inside a square cavity which is heated at two different temperature levels in the vertical walls. The use of RBFs followed by collocation resulted in a meshless formulation giving good results with very few collocation points when compared with the grids used for the classical benchmark solutions. For the lid-driven cavity problem, the mass and momentum equations are written in terms of vorticity and stream function which are thus rewritten as a bi-harmonic equation. The results were compared with those of Ghia et al. which used a grid with 129x129 volumes. With considerably fewer points, the RBFs were able to obtain a good result for the velocity profile. For the natural convection in a square cavity with the walls heated at different temperatures, the Boussinesq approximation was used and the bi-harmonic equation was solved coupled with the energy equation. The results were compared against those presented by de Vahl Davis who used a grid with 41x41 points and Leal et al. who solved this problem by using the Generalized Integral Transform Technique. Again, the RBF was able to obtain a reasonably good result with very few collocation points.*

Keywords*: Radial Basis Function, Lid-Driven Cavity, Natural Convection*

1. INTRODUCTION

The mathematical modeling of incompressible viscous flows is one of the classical problems in fluid mechanics, which has been studied by several authors over the past decades.

One of the main problems in dealing with incompressible flows is the absence of one equation for pressure, thus leading to the classical pressure-velocity coupling problem, where the pressure appearing in the momentum equation must generate velocity field that satisfies the mass conservation equation. Several approaches were developed in the past to deal with this problem such as the SIMPLE (Patankar and Spalding, 1972), SIMPLEC (Van Doormaal and Raithby, 1984), SIMPLER (Patankar, 1979) and PRIME (Maliska, 1981) methods.

Another well known problem encountered when solving the Navier-Stokes equations numerically, such as with Finite Volume Method, is the type of grid structure used, which can be co-located or staggered, depending on how the pressure and velocity fields are distributed along the control volumes. In the co-located grid structure, the velocity and pressure fields are all located at the centers of the control volumes. Thus, during the process of integrating the equations, several quantities must be evaluated at the boundary of such control volumes. The evaluation of such quantities at these interfaces is done by means of some interpolation scheme such as the Power-Law Scheme (Patankar, 1980), Upwind (Courant et al, 1952), WUDS (Raithby and Torrance, 1974), QUICK (Leonard, 1979) and QUICKEST (Leonard, 1979) among others (Leonard, 1997; Tafti, 1996).

Besides the two problems mentioned above, there is also the grid generation, which is, by itself, a fundamental part of the numerical solution of the governing equations for the incompressible viscous flow equations. The quality of the numerical solution depends on the grid size, grid uniformity, grid orthogonality and the grid smoothness. Complex geometries and multiply-connected domains can demand a large computational effort both to generate the grid and for solving the partial differential equations which model the physical problem. The computational cost might increase even more if solution-adaptive grids are used. To overcome the above mentioned difficulties, mesh-free and meshless methods have been developed over the past decades, seeking to avoid the drawbacks or weakness of the standard numerical methods, and yet preserve the ability to accommodate geometric complexity. From the viewpoint of kernel interpolation/approximation techniques, many mesh-free methods are based on the moving least square technique.

One of the most popular mesh-free kernel approximation techniques is Radial Basis Functions (RBFs). Initially, RBFs were developed for multivariate data and function interpolation. It was found that RBFs were able to construct an

interpolation scheme with favorable properties such as high efficiency, good quality and capability of dealing with scattered data, especially for higher dimensional problems. A good interpolation scheme also has great potential for solving partial differential equations. It was Kansa (1990) who made the first step forward in employing RBFs to deal with PDEs. He proposed a simple collocation method using RBFs.

Over the past decade, several problems were solved by using meshless methods. Chen *et al.* (2000, 2001, 2002) used the Boundary Knot Method (BKM) to solve some problems modeled by the Helmholtz and Laplace equations. Lavagetto *et al.* (2000) used the RBF as an interpolation function to recognize human faces. Ramachandran (2002) used the Method of Fundamental Solutions (MFS), which is also a meshless method, to solve equations such as the Laplace and Helmholtz equations. Scott (2004) used the RBF to solve the Burgers' equation and also investigated the use of an adaptive choice of the collocation points. Mera (2005) used the MFS to solve an inverse problem of heat conduction. Wu *et al.* (2005) studied the use of RBFs as interpolation functions, using the partition of unity method. Chen (2006) used the RBFs to solve the Poisson and Burgers' equations. Colaço *et al.* (2006) used the RBFs to solve some convection-diffusion problems, such as the Pouiseuille flow and the flow between two parallel plates. Several RBFs were compared, both using global and compact support. Chinchapatnam (2006) used the RBFs to solve the classical lid-driven cavity problem, where the problem was formulated as a bi-harmonic equation. Colaço *et al.* (2008) used RBFs as interpolation functions in a hybrid optimizer showing very good convergence rates. Vale *et al.* (2008) used the Method of Fundamental Solutions in an inverse heat transfer problem of estimating a heat transfer coefficient.

In this work, the natural convection problem in a square cavity was studied using Radial Basis Functions. Different Rayleigh numbers, as well as a different number and distribution of collocation points were employed.

2. RADIAL BASIS FUNCTIONS

Radial basis functions are essential ingredients of the techniques generally known as "meshless methods that require some sort of radial function to measure the influence of a given location on another part of the domain.

The use of Radial Basis Functions (RBF) followed by collocation, a technique first proposed by Kansa (Kansa, 1990), after the work of Hardy (Hardy, 1971) on multivariate approximation, is now becoming an established approach and various applications to problems of structures and fluids have been made in recent years – see, for example Leitão (Leitão, 2001; Leitão, 2004). Kansa's method (or asymmetric collocation) starts by building an approximation to the field of interest (normally displacement components) from the superposition of radial basis functions (globally or compactly supported) conveniently placed at points in the domain (and, or, at the boundary). The unknowns (which are the coefficients of each RBF) are obtained from the (approximate) enforcement of the boundary conditions as well as the governing equations by means of collocation. Usually, this approximation only considers regular radial basis functions, such as the globally supported multiquadrics or the compactly supported Wendland (Wendland, 1998) functions. Radial basis functions (RBFs) may be classified into two main groups:

1. the globally supported ones namelly the multiquadric (MQ, $\sqrt{(x-x_j)^2+c_j^2}$, where c_j is a shape parameter), the inverse multiquadric, thin plate splines, guassians, etc;
2. the compactly supported ones such as the Wendland (1998) family (for example, $(1-r)_+^n + p(r)$ where $p(r)$ is a polynomial and $(1-r)_+^n$ is 0 for r greater than the support).

In a very brief manner, interpolation with RBFs may take the form:

$$s(x_i) = f(x_i) = \sum_{j=1}^{N} \alpha_j \phi\left(\left|x_i - x_j\right|\right) + \sum_{k=1}^{\hat{N}} \beta_k p_k(x_i) \quad \text{subject to the conditions (for the sake of uniqueness)} \quad \sum_{j=1}^{N} \alpha_j p_k(x_j) = 0. \tag{1}$$

where $f(x_i)$ is known for a series of points x_i and $p_k(x_i)$ is one of the $\hat{N}$ terms of a given basis of polynomials, see Buhmann (Buhmann, 2003). This approximation is solved for the α_j unknowns from the system of N linear equations.

By using the same reasoning it is possible to extend the interpolation problem to that of finding the approximate solution of partial differential equations. This is made by applying the corresponding differential operators to the radial basis functions and then to use collocation at an appropriate set of boundary and domain points.

In short, the non-symmetrical collocation is the application of the domain and boundary differential operators *LI* and *LB*, respectively, to a set of *N-M* domain collocation points and *M* boundary collocation points.

From this, a system of linear equations of the following type may be obtained

$$\begin{aligned} LIu_h(x_i) &= \sum_{j=1}^{N} \alpha_j LI\phi\left(\left|x_i - \varepsilon_j\right|\right) + \sum_{k=1}^{\hat{N}} \beta_k LIp_k(x_i) \\ LBu_h(x_i) &= \sum_{j=1}^{N} \alpha_j LB\phi\left(\left|x_i - \varepsilon_j\right|\right) + \sum_{k=1}^{\hat{N}} \beta_k LBp_k(x_i) \end{aligned} \tag{2.a,b}$$

subject to the conditions $\sum_{j=1}^{N} \alpha_j p_k\left(x_j\right) = 0$ where the α_j and β_k unknowns are determined from the satisfaction of the domain and boundary constraints at the collocation points.

3. PHYSICAL PROBLEM

The physical problem considered here involves the laminar natural convection of an incompressible Newtonian fluid. The fluid physical properties are assumed constant. The energy source term resulting from viscous dissipation is neglected and buoyancy effects are approximated by the Boussinesq hypothesis. Radiative heat transfer is neglected. Figure 1 shows the geometry for this problem.

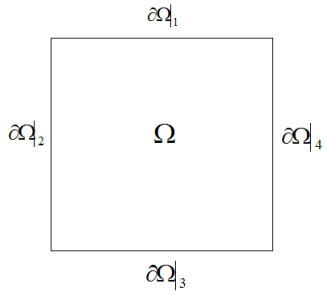

Figure 1 – Geometry and boundaries.

Equations (3.a-l) show the mathematical formulation of this problem. All boundaries are impenetrable and subjected to non-slip flow. Top and bottom boundaries are thermally insulated and vertical walls are subjected to different prescribed temperatures, which will give rise to the natural convection problem. In these equations, u and v are the components of the velocity field in the x and y coordinate directions, υ is the kinematic viscosity, ρ is the fluid viscosity, p is the pressure, T^* is the temperature, T_h is the temperature at the 'hot' surface and T_c is the temperature at the 'cold' surface.

$$\frac{\partial u}{\partial x} + \frac{\partial v}{\partial y} = 0 \qquad (x, y) \in \Omega \qquad (3.a)$$

$$u\frac{\partial u}{\partial x} + v\frac{\partial u}{\partial y} = \nu\left(\frac{\partial^2 u}{\partial x^2} + \frac{\partial^2 u}{\partial y^2}\right) - \frac{1}{\rho}\frac{\partial p}{\partial x} \qquad (x, y) \in \Omega \qquad (3.b)$$

$$u\frac{\partial v}{\partial x} + v\frac{\partial v}{\partial y} = \nu\left(\frac{\partial^2 v}{\partial x^2} + \frac{\partial^2 v}{\partial y^2}\right) - \frac{1}{\rho}\frac{\partial p}{\partial y} + g\beta(T^* - T_C) \qquad (x, y) \in \Omega \qquad (3.c)$$

$$u\frac{\partial T^*}{\partial x} + v\frac{\partial T^*}{\partial y} = \alpha\left(\frac{\partial^2 T^*}{\partial x^2} + \frac{\partial^2 T^*}{\partial y^2}\right) \qquad (x, y) \in \Omega \qquad (3.d)$$

$$u = v = 0 \qquad \frac{\partial T^*}{\partial y} = 0 \qquad \text{at } \partial\Omega|_1 \qquad (3.e,f)$$

$$u = v = 0 \qquad T = T_H \qquad \text{at } \partial\Omega|_2 \qquad (3.g,h)$$

$$u = v = 0 \qquad \frac{\partial T^*}{\partial y} = 0 \qquad \text{at } \partial\Omega|_3 \qquad (3.i,h)$$

$$u = v = 0 \qquad T = T_C \qquad \text{at } \partial\Omega|_4 \qquad (3.k,l)$$

The above equations can be simplified with the help of the stream function formulation

$$u = \frac{\partial \psi}{\partial y} \qquad v = -\frac{\partial \psi}{\partial x} \qquad (4.a,b)$$

It is possible also to define the following dimensionless variables, as well as the Prandtl and Rayleigh numbers

$$X=\frac{x}{D} \quad Y=\frac{y}{D} \quad \Psi=\frac{\psi}{\nu} \quad T=\frac{T^*-T_C}{T_H-T_C} \quad \mathrm{Pr}=\frac{\nu}{\alpha} \quad \mathrm{Ra}=\frac{g\beta(T_H-T_C)D^3}{\nu\alpha} \tag{5.a-f}$$

where D is the length of the cavity, α is the thermal diffusivity, g is the gravity vector at the y direction and β is the volumetric coefficient of thermal expansion.

Substituting Eqs. (4) and (5) into Eqs. (3), it is possible to obtain, after some manipulation, the following equations

$$\left[\frac{\partial^4\Psi}{\partial X^4}+2\frac{\partial^4\Psi}{\partial X^2\partial Y^2}+\frac{\partial^4\Psi}{\partial Y^4}\right]-\left[\frac{\partial\Psi}{\partial Y}\left(\frac{\partial^3\Psi}{\partial X^3}+\frac{\partial^3\Psi}{\partial X\partial Y^2}\right)-\frac{\partial\Psi}{\partial X}\left(\frac{\partial^3\Psi}{\partial Y^3}+\frac{\partial^3\Psi}{\partial X^2\partial Y}\right)\right]-\frac{\mathrm{Ra}}{\mathrm{Pr}}\frac{\partial T}{\partial X}=0 \tag{6.a}$$

$$\frac{\partial\Psi}{\partial Y}\frac{\partial T}{\partial X}-\frac{\partial\Psi}{\partial X}\frac{\partial T}{\partial Y}=\frac{1}{\mathrm{Pr}}\left(\frac{\partial^2 T}{\partial X^2}+\frac{\partial^2 T}{\partial Y^2}\right) \tag{6.b}$$

$$\Psi=0,\frac{\partial\Psi}{\partial Y}=0 \qquad \frac{\partial T}{\partial Y}=0 \qquad \text{at } \partial\Omega\big|_1 \tag{6.c-e}$$

$$\Psi=0,\frac{\partial\Psi}{\partial X}=0 \qquad T=1 \qquad \text{at } \partial\Omega\big|_2 \tag{6.f-h}$$

$$\Psi=0,\frac{\partial\Psi}{\partial Y}=0 \qquad \frac{\partial T}{\partial Y}=0 \qquad \text{at } \partial\Omega\big|_3 \tag{6.i-k}$$

$$\Psi=0,\frac{\partial\Psi}{\partial X}=0 \qquad T=0 \qquad \text{at } \partial\Omega\big|_4 \tag{6.l-n}$$

Equation (6.a) is a bi-harmonic equation with a source term given by the temperature gradient along the dimensionless X coordinate. Equations (6.a) and (6.b) must be solved simultaneously due to the presence of such source term. As the Rayleigh number increases or the Prandtl number decreases, the coupling among the two equations becomes stronger. For a Rayleigh number equals to zero, both equations can be solved independently. It is interesting to note that the gradient of pressure no longer appears in such equations, thus eliminating the pressure-velocity coupling problem mentioned before. The presence of fourth order derivatives in Eqs. (6.a) and (6.b) makes their solution highly prone to truncation errors when numerical techniques such as finite differences of finite volumes are applied to them. The need for three boundary conditions at each one of the boundaries, as given by Eqs. (6.c-n), should be pointed out.

4. SOLUTION TECHNIQUE

In this work we used the Radial Basis Function to solve the natural convection problem within a square cavity. Several choices of RBFs are possible (Colaco, 1996). In this work, we used the multiquadrics, because of its simplicity, low computational cost and overall good accuracy. The variables appearing on Eqs. (6) were thus expanded by using a RBF approximation as

$$\Psi(X,Y)=\sum_{i=1}^{N}\lambda_i\varphi_i(r_i) \qquad T(X,Y)=\sum_{j=1}^{M}\lambda_j\varphi_j(r_j) \tag{7.a,b}$$

where

$$\varphi(\mathbf{r}_i)=\sqrt{\mathbf{r}_i}=\sqrt{(x-x_i)^2+(y-y_i)^2+c_i} \tag{8}$$

In the above equations, the functions φ are the same for both variables Ψ and T, but the parameters λ are different for each one. The variable c is a shape parameter that controls the smoothness of the RBF. As c becomes large, the RBF becomes smoother, the solution becomes better, but the resulting linear system is ill-conditioned. In these equations, N and M are the number of collocation points, which are different for the two variables and will be explained later. Applying Eqs. (7) and (8) into Eqs. (6), the following non-linear system was obtained which need to be solved for λ. The non-linear system given by Eqs. (9) was solved by the BFGS Method (Press et al, 1999). After the solution of Eqs. (9), the final value of the stream-function and the temperature can be recovered by Eqs. (7.a) and (7.b), respectively.

$$\left[\sum_{i=1}^{N}\lambda_i\frac{\partial^4\varphi_i}{\partial X^4}+2\sum_{i=1}^{N}\lambda_i\frac{\partial^4\varphi_i}{\partial X^2\partial Y^2}+\sum_{i=1}^{N}\lambda_i\frac{\partial^4\varphi_i}{\partial Y^4}\right]- \tag{9.a}$$
$$\left[\sum_{i=1}^{N}\lambda_i\frac{\partial\varphi_i}{\partial Y}\left(\sum_{i=1}^{N}\lambda_i\frac{\partial^3\varphi_i}{\partial X^3}+\sum_{i=1}^{N}\lambda_i\frac{\partial^3\varphi_i}{\partial X\partial Y^2}\right)-\sum_{i=1}^{N}\lambda_i\frac{\partial\varphi_i}{\partial X}\left(\sum_{i=1}^{N}\lambda_i\frac{\partial^3\varphi_i}{\partial Y^3}+\sum_{i=1}^{N}\lambda_i\frac{\partial^3\varphi_i}{\partial X^2\partial Y}\right)\right]$$
$$-\frac{\mathrm{Ra}}{\mathrm{Pr}}\sum_{j=1}^{M}\lambda_j\frac{\partial\varphi_j}{\partial X}=0$$

$$\sum_{i=1}^{N}\lambda_i\frac{\partial\varphi_i}{\partial Y}\sum_{j=1}^{M}\lambda_j\frac{\partial\varphi_j}{\partial X}-\sum_{i=1}^{N}\lambda_i\frac{\partial\varphi_i}{\partial X}\sum_{j=1}^{M}\lambda_j\frac{\partial\varphi_j}{\partial Y}=\frac{1}{\mathrm{Pr}}\left(\sum_{j=1}^{M}\lambda_j\frac{\partial^2\varphi_j}{\partial X^2}+\sum_{j=1}^{M}\lambda_j\frac{\partial^2\varphi_j}{\partial Y^2}\right) \tag{9.b}$$

$$\sum_{i=1}^{N}\lambda_i\varphi_i=0,\sum_{i=1}^{N}\lambda_i\frac{\partial\varphi_i}{\partial Y}=0 \qquad \sum_{j=1}^{M}\lambda_j\frac{\partial\varphi_j}{\partial Y}=0 \qquad \text{at } \partial\Omega\big|_1 \tag{9.c-e}$$

$$\sum_{i=1}^{N}\lambda_i\varphi_i=0,\sum_{i=1}^{N}\lambda_i\frac{\partial\varphi_i}{\partial X}=0 \qquad \sum_{j=1}^{M}\lambda_j\varphi_j=1 \qquad \text{at } \partial\Omega\big|_2 \tag{9.f-h}$$

$$\sum_{i=1}^{N}\lambda_i\varphi_i=0,\sum_{i=1}^{N}\lambda_i\frac{\partial\varphi_i}{\partial Y}=0 \qquad \sum_{j=1}^{M}\lambda_j\frac{\partial\varphi_j}{\partial Y}=0 \qquad \text{at } \partial\Omega\big|_3 \tag{9.i-k}$$

$$\sum_{i=1}^{N}\lambda_i\varphi_i=0,\sum_{i=1}^{N}\lambda_i\frac{\partial\varphi_i}{\partial X}=0 \qquad \sum_{j=1}^{M}\lambda_j\varphi_j=0 \qquad \text{at } \partial\Omega\big|_4 \tag{9.l-n}$$

At this point, it is necessary to explain why M and N must be different. Let us suppose that we have L point inside the domain, which are given by the blue dots in Fig. 2. Also, we have P points at the boundaries, given by the green dots at the same figure. Starting with the energy equation (9.b), we will have one equation for each one of the blue centers shown in the Fig. 2. Besides, the boundary conditions (9.e), (9.h), (9.k) and (9.n) will be applied to the boundary points given by the green centers. Thus, the total number of equations is $L+P$, which is equal to the total number of variables M in Eq. (7.b). Since we have one equation applied to different points, the number of variables and equations are the same and the system is determined. However, let us now analyze the bi-harmonic equation. Equation (9.a) gives one equation for each internal point of the domain (blue dots in Fig. 2) and Eqs. (9.c), (9.d), (9.f), (9.g), (9.i), (9.j), (9.l) and (9.m) results in two equations for each point of the boundaries (green dots in Fig. 2). Therefore, the total number of equations for the stream-function is $L+2*P$, which is equal to N. However, the total number of variables is $L+P$. In order to circumvent this, it is necessary to introduce more variables in the system. In this work, we followed the approach used by Chinchapatnam (2006), who used some ghost centers (red dots in Fig. 2) outside the domain and close to the boundary conditions. Thus, some extra centers are introduced making the system determined. Note that the equations are not solved for these centers. They appear only as extra variables λ_i.

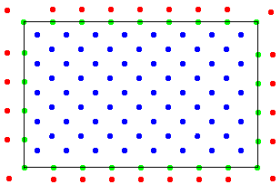

Figure 2 – Collocation points (blue=domain centers, green=boundary centers, red=ghost centers)

An important issue when using RBFs to solve a system of partial differential equations is related to the choice of the shape parameter c appearing in Eq. (8). The quality of the results is greatly influenced by this choice. As the shape parameter increases, the solution usually is better at the cost of an ill-conditioned system of algebraic equations. Divo and Kassab (2007) suggest a trial and error approach, where the shape parameter must be increased up to the point where the system is almost unsolvable. Following the suggestions of Chinchapatnam (2006) we first determined the lowest distance among all internal points of the domain and called this distance d. Then, the non-linear system given by Eqs. (9) was solved for $c = d$ and the residual was recorded. The entire procedure was repeated, but for $c = 2d$ and a new residual was recorded. This process was repeated for c equals to up five times d and the best shape parameter was the one that gave the lowest residual in the solution of Eqs. (9). Note that this system is generally ill-conditioned. Thus, the initial guess for each new value of c was taken as the solution of the previous step. This entire procedure was repeated again five times, in order to guarantee that the initial guesses no longer influenced the final solution and the best value of c was finally obtained.

5. RESULTS AND DISCUSSION

The natural convection problem in a square cavity was analyzed for three different Rayleigh numbers (10^4, 10^5 and 10^6) and the numerical results were compared against the benchmark results of Vahl Davis (1983) and Leal *et al.* (1999). While Vahl Davis (1983) used a numerical technique to obtain his results, Leal et al (1999) used the Generalized Integral Transform Technique to solve this problem. In this work we used 16, 64, 144, 256, 400, 900 and 1600 collocation points in order to verify the convergence of the results as the number of points was increased. In all comparisons, the Prandlt number was taken as 0.71, since it was the one used in the benchmark results. Besides the multiquadrics given by Eq. (8), other types of RBFs were tried, such as the Gaussian (Buhmann, 2003) and the ones with compact support (Wendland, 1998). However, only the results obtained through the use of the multiquadrics will be presented, since they resulted in the better agreement with the benchmark results.

Figure 3 shows a qualitative comparison among the current results and the ones presented by Vahl Davis (1983) for the stream-function, isothermals and lines of constant vorticity. For these results we used 1600 collocation points and three different Rayleigh numbers were analyzed. From this figure, it is clear that the distribution of stream-function, isothermals and lines of constant vorticity are in good agreement with the benchmark results.

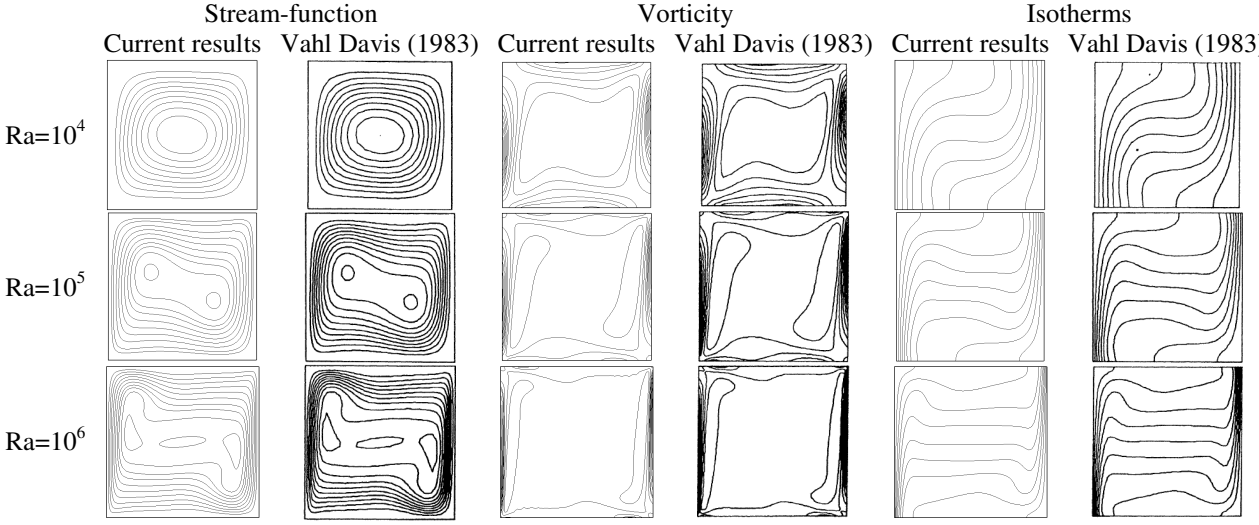

Figure 3 – A qualitative comparison against the results of Vahl Davis (1983).

In order to provide a better analysis of the results, we compared the current results against the one presented by Leal *et al.* (1999). In their paper, Leal *et al.* (1999) provided results for the maximum value of the component *U* of the velocity field along the half height of the cavity and its location, as well as the maximum value of the component *V* of the velocity field along the half width of the cavity and its location. Other parameters were also analyzed, which are given by Eqs. (10).

$$Nu_X = \int_0^1 \left\{ \frac{\partial \Psi}{\partial Y} T - \frac{\partial T}{\partial X} \right\} dY \tag{10.a}$$

$$\overline{Nu} = \int_0^1 Nu_X \, dX \tag{10.b}$$

$$Nu_{\max} = \left\{ \frac{\partial \Psi}{\partial Y} T - \frac{\partial T}{\partial X} \right\} \Big|_{Maximum\ at\ X=0} \tag{10.c}$$

$$Nu_{\min} = \left\{ \frac{\partial \Psi}{\partial Y} T - \frac{\partial T}{\partial X} \right\} \Big|_{Minimum\ at\ X=0} \tag{10.d}$$

$$Nu_{1/2} = \{ Nu_X \}_{X=1/2} \tag{10.e}$$

$$Nu_0 = \{ Nu_X \}_{X=0} \tag{10.f}$$

Table 1 shows the comparison against the results of Leal *et al.* (1999) for the parameters discussed previously for several sizes of collocation points *N* equally distributed. In this table, the errors ε among the current results and the ones

presented by Leal *et al.* (1999) are also presented. As one can see, the relative errors between the two solutions decrease as the number of collocation points N increases. Even for a relatively small number of collocation points, such as N = 144, most of the parameters had errors less than 3%, except the Nu_{max} and Nu_{min} and their locations. For 1600 collocation points, the relative errors were less than 1% for all parameters, except for Nu_{max} and Nu_{min} and their locations, which reached errors less than 9%. This suggests that probably there is the necessity to locate some points close to the boundaries, since the worst parameters were the ones located at $X = 0$. This will be discussed later.

Table 1 – Comparison against the results of Leal *et al.* (1999) for Ra = 10^4

Ra=10^4	Leal et al (1999)	N=16	ε%	N=64	ε%	N=144	ε%	N=256	ε%	N=400	ε%	N=900	ε%	N=1600	ε%
U_{max}	16.180	13.208	18.4	15.412	4.7	15.795	2.4	15.999	1.1	16.055	0.8	16.065	0.7	16.122	0.4
Y	0.823	0.810	1.6	0.820	0.4	0.820	0.4	0.820	0.4	0.820	0.4	0.820	0.4	0.820	0.4
V_{max}	19.630	16.125	17.8	19.004	3.2	19.349	1.4	19.447	0.9	19.510	0.6	19.526	0.5	19.577	0.3
X	0.119	0.150	26.0	0.120	0.8	0.120	0.8	0.120	0.8	0.12	0.8	0.12	0.8	0.12	0.8
$\overline{Nu}$	2.245	1.956	12.9	2.244	0.04	2.250	0.2	2.248	0.1	2.247	0.1	2.248	0.1	2.246	0.1
Nu_0	2.245	3.390	51.0	2.482	10.5	2.310	2.9	2.255	0.4	2.251	0.3	2.236	0.4	2.241	0.2
$Nu_{1/2}$	2.245	1.715	23.6	2.192	2.3	2.216	1.3	2.232	0.6	2.235	0.4	2.232	0.6	2.239	0.3
Nu_{max}	3.532	5.123	45.0	4.362	23.5	3.815	8.0	3.586	1.5	3.556	0.7	3.521	0.3	3.524	0.2
Y	0.143	0.000	>100	0.000	>100	0.000	>100	0.060	>100	0.130	9.0	0.10	30.0	0.130	9.0
Nu_{min}	0.585	1.586	>100	0.550	6.0	0.612	4.6	0.598	2.2	0.597	2.0	0.620	6.0	0.600	2.6
Y	1.000	1.000	0.0	1.000	0.0	1.000	0.0	1.000	0.0	1.000	0.0	1.000	0.0	1.000	0.0

Table 2 shows the comparison against the results of Leal *et al*. (1999) for the Rayleigh number equals to 10^5. Again, as the number of collocation points N increases, the current results become closer to the benchmark ones. However, since the buoyancy forces are stronger than in the case with Ra = 10^4, making Eqs. (9.a) and (9.b) more coupled; the relative errors are slightly higher than the ones presented in Table 1. For 1600 collocation points, most of the relative errors are close to 1% and the Nu_{max} and Nu_{min} and their locations had errors up to 13.6 %. Again, the use of a non uniform distribution of collocation points shall be analyzed in order to verify its effect on the relative errors of Nu_{max} and Nu_{min} and their locations.

Table 2 – Comparison against the results of Leal *et al.* (1999) for Ra = 10^5

Ra=10^5	Leal et al. (1999)	N=16	ε%	N=64	ε%	N=144	ε%	N=256	ε%	N=400	ε%	N=900	ε%	N=1600	ε%
U_{max}	34.740	29.509	15.1	27.735	20.2	30.979	10.8	32.922	5.2	33.715	2.9	34.283	1.3	34.453	0.8
Y	0.855	0.840	1.7	0.840	1.7	0.840	1.7	0.850	0.6	0.850	0.6	0.850	0.6	0.850	0.6
V_{max}	68.620	42.961	37.4	57.290	16.5	64.471	6.0	67.088	2.2	67.772	1.2	67.983	0.9	68.252	0.5
X	0.066	0.130	96.9	0.080	21.2	0.070	6.0	0.070	6.0	0.07	6.0	0.07	6.0	0.07	6.0
$\overline{Nu}$	4.522	2.332	48.4	3.811	15.7	4.339	4.0	4.478	0.9	4.511	0.2	4.521	0.1	4.521	0.1
Nu_0	4.522	5.589	23.6	6.498	43.7	5.744	27.0	5.091	12.6	4.761	5.3	4.551	0.6	4.522	0.0
$Nu_{1/2}$	4.522	1.799	60.2	3.616	20.0	4.269	5.6	4.443	1.8	4.488	0.7	4.508	0.3	4.512	0.2
Nu_{max}	7.721	6.969	9.7	10.876	40.8	11.22	45.3	10.267	32.9	9.270	20.0	8.110	5.0	7.828	1.4
Y	0.081	0.020	75.3	0.020	75.3	0.000	>100	0.000	>100	0.000	>100	0.03	62.9	0.07	13.6
Nu_{min}	0.728	3.908	>100	2.139	>100	0.942	29.4	0.777	6.7	0.768	5.5	0.762	4.7	0.756	3.8
Y	1.000	1.000	0.0	1.000	0.0	1.000	0	1.000	0.0	1.000	0.0	0.970	3.0	0.980	2.0

Finally, Table 3 shows the comparison among the current results and the ones presented by Leal *et al.* (1999) for Ra = 10^6. Comparing Table 3 with Tables 1 and 2 it is clear that as the buoyancy effects increase, the solution becomes worst for the same number of collocation points. Once again, the worst results were obtained for Nu_{max} and Nu_{min} and their locations, which are variables evaluated at the boundary of the cavity. A non-uniform distribution of collocation points will be presented next, where these difficulties will be partially circumvented.

Table 3 – Comparison against the results of Leal *et al.* (1999) for Ra = 10^6

Ra=10^6	Leal et al. (1999)	N=16	ε%	N=64	ε%	N=144	ε%	N=256	ε%	N=400	ε%	N=900	ε%	N=1600	ε%
U_{max}	64.830	197.575	>100	56.276	13.2	50.625	21.9	54.475	15.9	57.684	11.0	62.013	4.3	63.521	2.0
Y	0.850	0.730	14.1	0.860	1.18	0.850	0.0	0.850	0.0	0.850	0.0	0.850	0.0	0.850	0.0
V_{max}	220.600	550.635	>100	143.772	34.8	168.064	23.8	186.937	15.2	201.121	8.8	217.315	1.5	218.305	1.0
X	0.038	0.290	>100	0.070	84.2	0.050	31.6	0.040	5.3	0.040	5.3	0.040	5.2	0.040	5.3
$\overline{Nu}$	8.825	8.608	2.46	4.604	47.8	6.458	26.8	7.545	14.5	8.162	7.5	8.679	1.6	8.798	0.3
Nu_0	8.826	1.069	87.9	9.868	11.8	11.744	33.1	11.985	35.8	11.516	30.5	9.895	12.1	9.221	4.5
$Nu_{1/2}$	8.825	1.627	81.6	4.112	53.4	6.198	29.7	7.396	16.2	8.081	8.4	8.645	2.0	8.784	0.5
Nu_{max}	17.540	28.981	65.2	13.987	20.2	20.145	14.8	23.605	34.6	25.220	43.8	24.558	40.0	22.135	26.2
Y	0.039	0.630	>100	0.020	48.7	0.020	48.7	0.010	74.3	0.010	74.3	0.000	>100	0.000	>100
Nu_{min}	0.979	-25.526	>100	5.523	>100	3.903	>100	2.015	>100	1.183	20.8	0.982	0.3	0.970	0.9
Y	1.000	0.770	23.0	0.900	10.0	0.940	6.0	0.950	5.0	0.960	4.0	0.970	3.0	0.980	2.0

Finally, table 4 shows the computational time required for the solution of the natural convection problem in a square cavity using the RBF approach presented in this work, for a uniform distribution of collocation points. The codes were developed in Fortran 90 and compiled using the version 6.6.0 of the Compaq Visual Fortran. All codes ran in a Pentium IV 3.06Ghz with 1.0Gb of RAM memory. From this table, one can see that the computational time varied from a few seconds to several hours. A further investigation on the use of more efficient solvers for the non-linear system resulting from the application of the RBFs shall be investigated. A large amount of CPU time is indeed consumed during the choice of the shape parameter c, as discussed previously. In fact, more efficient algorithms to chose the best shape parameter shall be developed in the future in order to make the use of the RBFs more competitive against classical numerical, analytical and hybrid methods.

Table 4 – CPU time required for the solution using RBF

	CPU time		
N	Ra=10^4	Ra=10^5	Ra=10^6
16	0.2s	0.7s	3.6s
64	2.5s	4.3s	9.5s
144	18.5s	33.9s	66.6s
256	77.1s	111.7s	213.4s
400	198.4s (3.3 min.)	321.3s (5.4 min.)	709.3s (11.8 min.)
900	2354.9s (39.2 min.)	5075.3s (84.6 min.)	6299.0s (105.0 min.)
1600	24241.8s (6.7 hours)	21815.6s (6.1 hours)	42695.0s (11.9 hours)

As discussed above, some results with a non-uniform distribution of collocation points will be now presented for the three Rayleigh numbers analyzed in this paper. A dimensionless factor ξ was used to approximate the collocation points to the boundaries of the cavity. Besides the uniform distribution, four other distributions were analyzed, as shown in Fig. 4, depending on how big is such dimensionless factor.

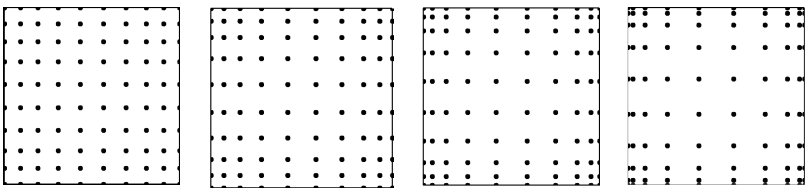

Figure 4 – Different non-uniform distribution of collocation points for (a)ξ=0.2, (b)ξ=0.4, (c)ξ=0.6 and (d)ξ=0.8

Table 5 shows the results obtained when a non-uniform distribution of collocation points was used. In this table, only the results obtained with the best value of the dimensionless factor ξ are presented. Thus, for Ra=10^4, the best value of ξ was 0.2, for Ra=10^5 ξ = 0.4 gave the best results and for Ra=10^6, the best results were obtained with ξ equals to 0.2.

The results are presented only for N = 1600. Comparing the results presented in Table 5 with the ones presented in Tables 1, 2 and 3 it is clear that the solution became more accurate when a non-uniform distribution of collocation points was used. For a Rayleigh number equal to 10^4, comparing the last two columns of Table 1 with the results in Table 5, all relative errors decrease, specially the ones related to the Y location of the Nu_{max}, which decrease from 9.0% to 2.1%. Also, comparing the results presented in the last two columns of Table 2, for Ra = 10^5, with the ones of Table 5 the relative errors also decreased. Note that the Y location of the Nu_{max}, which had an error equal to 13.6% for a uniform distribution of collocation points, now have an error equal to 1.2%, when a non-uniform distribution was used. For Ra = 10^6, the solution did not improve for all parameters, as one can verify by inspecting the last two columns of Table 3 and the Table 5. Although the relative error for some variables decreases, such as the Nu_{max}, some other values had errors worse than before, such as the Nu_{min}. This suggests that a further investigation concerning the distribution of the collocation points shall be investigated.

Table 5 – Comparison against the results of Leal *et al.* (1999) for non-uniform distribution of collocation points

Ra=10^4 ξ=0.2	Leal et al. (1999)	N=1600	ε%	Ra=10^5 ξ=0.4	Leal et al. (1999)	N=1600	ε%	Ra=10^6 ξ=0.2	Leal et al. (1999)	N=1600	ε%
U_{max}	16.180	16.136	0.3	U_{max}	34.740	34.622	0.3	U_{max}	64.830	64.006	1.3
Y	0.823	0.82	0.4	Y	0.855	0.85	0.6	Y	0.850	0.85	0.0
V_{max}	19.630	19.585	0.2	V_{max}	68.620	68.368	0.4	V_{max}	220.600	218.28	1.1
X	0.119	0.12	0.8	X	0.066	0.07	6.1	X	0.038	0.04	5.3
$\overline{Nu}$	2.245	2.246	0.0	$\overline{Nu}$	4.522	4.521	0.0	$\overline{Nu}$	8.825	8.81	0.2
Nu_0	2.245	2.239	0.3	Nu_0	4.522	4.515	0.2	Nu_0	8.826	8.957	1.5
$Nu_{1/2}$	2.245	2.24	0.2	$Nu_{1/2}$	4.522	4.517	0.1	$Nu_{1/2}$	8.825	8.795	0.3
Nu_{max}	3.532	3.52	0.3	Nu_{max}	7.721	7.735	0.2	Nu_{max}	17.540	20.438	16.5
Y	0.143	0.14	2.1	Y	0.081	0.08	1.2	Y	0.039	0	>100
Nu_{min}	0.585	0.6	2.6	Nu_{min}	0.728	0.741	1.8	Nu_{min}	0.979	1.025	4.7
Y	1.000	1	0.0	Y	1.000	1	0.0	Y	1.000	0.98	2.0

6. CONCLUSIONS

In this paper we applied the Radial Basis Function (RBF) method to the solution of the classical natural convection problem in a square cavity. Three Rayleigh numbers were tested in order to verify the accuracy of the method when the coupling among the momentum and energy equation was stronger. Different sizes and distributions of collocation points were used and an iterative procedure to determine the optimum value of the shape parameter, used in the RBF approach, was presented. The results show that the RBFs provided good estimates of the velocity and temperature fields when compared to two benchmark solutions. Further investigations shall be made concerning: (i) the choice of the shape parameters; (ii) the solution of the non-linear system resulting from the use of the RBFs which is very ill-conditioned; and (iii) the adaptive location of the collocation points.

7. ACKNOWLEDGEMENTS

This work was partially funded by CNPq, CAPES and FAPERJ (Brazilian councils for scientific development). M. J. Colaço is very grateful to the financial support from FIU as well as the hospitality of the Dulikravich's family during his staying in Miami from September to November of 2006, April of 2007 and January of 2008. The authors would also like to thank Profs. Carlos Alves and Vitor Leitão from Instituto Superior Técnico of Portugal, who first introduced to them the concepts of the RBFs. This work was also partially sponsored by the US Air Force Office of Scientific Research under grant FA9550-06-1-0170 monitored by Dr. Todd E. Combs, Dr. Fariba Fahroo and Dr. Donald Hearn and by the US Army Research Office/Materials Division under the contract number W911NF-06-1-0328 monitored by Dr. William M. Mullins. The views and conclusions contained herein are those of the authors and should not be interpreted as necessarily representing the official policies or endorsements, either expressed or implied, of the US Air Force Office of Scientific Research, the US Army Research Office or the U.S. Government. The U.S. Government is authorized to reproduce and distribute reprints for government purposes notwithstanding any copyright notation thereon.

8. REFERENCES

Buhmann, M.D., 2003, "Radial Basis Functions on Grids and Beyond", International Workshop on Meshfree Methods, Lisbon, Portugal.

Chen, C.S., 2006, "Meshless Methods for Scientific Computation", Department of Mathematical Sciences, University of Nevada, Las Vegas, U.S.A..

Chen, W. and Hon, Y.C., 2001, "Boundary knot method for 2D and 3D Helmholtz and convection-diffusion problems under complicated geometry", Int. J. Numer. Methods Engng, Vol. 56, Iss. 13, pp. 1931-1948.

Chen, W. and Tanaka, M., 2002, "A meshless, integration-free, and boundary-only RBF technique", Computers and Mathematics with Applications, 43, pp.379-391.

Chen, W. and Tanaka, M., 2000, "New advances in dual reciprocity and boundary-only RBF methods", BEM Technique Conference, Vol. 10, pp.17-22, Tokyo, Japan.

Chinchapatnam, P.P., Djidjeli, K. and Nair, P. B., 2006, "Meshless RBF Collocation for Steady Incompressible Viscous Flows", 36th AIAA Fluid Dynamics Conference and Exhibit, San Francisco, California, Jun 5-8.

Colaço, M.J., Dulikravich, G.S. and Sahoo, D., 2008, "A Response Surface Method Based Hybrid Optimizer", Inverse Problems in Science and Engineering (to appear).

Valle, M.F., Colaço, M.J. and Scofano Neto, F., 2008, "Estimation of the Heat Transfer Coefficient by Means of the Method of Fundamental Solutions", Inverse Problems in Science and Engineering (to appear).

Colaço, M.J., Orlande H. R. B., Roberty, N. C., Alves, C. and Leitão, V., 2006, "On The Solution of Diffusion-Convection Problems by Means of RBF Approximations", Proceedings of the 11th Brazilian Congress of Thermal Sciences and Engineering – ENCIT, ABCM, Curitiba, Brazil, December 5-8.

Courant, R., Isaacson, E. and Rees, M., 1952, "On the Solution of Non-Linear Hyperbolic Differential Equations by Finite Differences", Comm. Pure Appl. Math., Vol. 5, pp. 243.

Divo, E. and Kassab, A.J., 2007, An Efficient Localized Radial Basis Function Meshless Method for Fluid Flow and Conjugate Heat Transfer". ASME Journal of Heat Transfer, Vol. 129 (2), pp. 124-136.

Hardy, R.L., 1971, "Multiquadric Equations of Topography and Other Irregular Surfaces", Journal of Geophysics Res., Vol. 176, pp. 1905-1915.

Kansa, E.J., 1990, "Multiquadrics – A Scattered Data Approximation Scheme with Applications to Computational Fluid Dynamics – II: Solutions to Parabolic, Hyperbolic and Elliptic Partial Differential Equations", Comput. Math. Applic., Vol. 19, pp. 149-161.

Lavagetto, F., Pockaj, R. and Costa, M., 2000, "Smooth surface interpolation and texture adaptation for MPEG-4 compliant calibration of 3D head models", Image and Vision Computing 18, pp.345–353.

Leal, M.A., Pérez-Guerrero, J.S. and Cotta, R.M., 1999, "Natural convection inside two-dimensional cavitities: The integral transform method", Communications in Numer. Meth. Eng., Vol. 15, pp. 113-125.

Leitão, V.M.A., 2001, "A Mesheless Method for Kirchhoff Plate Bending Problems", International Journal of Numerical Methods in Engineering, Vol. 52, pp. 1107-1130.

Leitão, V.M.A., 2004, "RBF-Based Meshless Methods for 2D Elastostatic Problems", Engineering Analysis with Boundary Elements, Vol. 28, pp. 1271-1281.

Leonard, B.P., 1997, Advances in Numerical Heat Transfer, Vol. 1, Chapter 1, Bounded High-Order Upwind Multidimensional Finite-Volume Convection-Diffusion Algorithms, pp. 1-57, Taylor & Francis.

Leonard, B.P., 1979, "A Stable and Accurate Convective Modelling Procedure Based on Quadratic Upstream Interpolation", Comput. Methods Appl. Mech. Engrg., Vol. 19, pp. 59-98.

Leonard, B.P., MacVean, M.K. and Lock, A.P., 1995, "The Flux Integral Method for Multidimensional Convection and Diffusion", Appl. Math. Modelling, Vol. 19, pp. 333-342.

Maliska, C.R., 1981, "A Solution Method for Three-Dimensional Parabolic Fluid Flow Problems in Nonorthogonal Coordinates", Ph.D. Thesis, University of Waterloo, Waterloo, Canada.

Mera, N.S., 2005, "The method of fundamental solutions for the backward heat conduction problem", Inverse Problems in Science and Engineering, Vol. 13, No 1, pp 13, 1, pp.79-98.

Patankar, S.V., 1979, "A Calculation Procedure for Two-Dimensional Elliptic Situations", Numerical Heat Transfer, Vol. 2, pp. 409-425.

Patankar, S.V., 1980, Numerical Heat Transfer and Fluid Flow, Computational Method in Mechanics and Thermal Sciences, Hemisphere Publishing Corporation.

Patankar, S.V. and Spalding, D.B., 1972, "A Calculation Procedure for Heat, Mass and Momentum Transfer in Three-Dimensional Parabolic Flows", International Journal of Heat and Mass Transfer, Vol. 15, pp. 1787.

Press, W.H., Teukolsky, S.A., Vetterling, W.T. and Flannery, B.P., 1999, Numerical Recipes in Fortran 77.

Raithby, G.D. and Torrance, K.E., 1974, "Upstream-Weighted Differencing Schemes and Their Applications to Elliptic Problems Involving Fluid Flow", Computers & Fluids, Vol. 2, pp. 191-206.

Ramachandran, P.A., 2002, "Method of Fundamental Solutions: Singular Value Decomposition Analysis", Communications in numerical methods in engineering, pp. 789-801.

Scott, A.S., 2004, "Adaptive Radial Basis Function Methods for Time Dependent Partial Differential Equations", Applied Numerical Mathematics,Vol. 54, pp. 79-94.

Tafti, D., 1996, "Comparison of Some Upwind-Based High-Order Formulations with a Second-Order Central-Difference Scheme for Time Integration of the Incompressible Navier-Stoker Equations", Computer & Fluids, Vol. 25, Iss. 7, pp. 647-665.

Vahl Davis, G., 1983, "Natural convection of air in a square cavity: A benchmark numerical solution", Int. J. Numer. Methods Fluids, Vol. 3, pp. 249-264.

Van Doormaal, J.P. and Raithby, G.D., 1984, "Enhancements of the SIMPLE Method for Predicting Incompressible Flow", Numerical Heat Transfer. Vol. 7, pp. 147-163.

Wendland, H., 1998, "Error Estimates for Interpolation by Compactly Supported Radial Basis Functions of Minimal Degree", Journal of Approximation Theory, Vol. 93, pp. 258-272.

Wu, X., Wang, M.Y. and Xia, Q., 2005, "Implicit Fitting and Smoothing Using Radial Basis Functions with Partition of Unity", 9th International Conference on Computer Aided Design and Computer Graphics, pp. 139-148, Hong Kong, China, December 7-10.